Foot flexibility confounds the assessment of triceps surae extensibility in children with spastic paresis during typical physical examinations

Weide, Guido; Huijing, Peter A.; Becher, Jules G.; Jaspers, Richard T.; Harlaar, Jaap

Important note
To cite this publication, please use the final published version (if applicable).
Please check the document version above.

Foot flexibility confounds the assessment of triceps surae extensibility in children with spastic paresis during typical physical examinations

Guido Weide [a,b], Peter A. Huijing [a], Jules G. Becher [b], Richard T. Jaspers [a], Jaap Harlaar [b,c,*]

[a] Laboratory for Myology, Dept. of Human Movement Sciences, Amsterdam Movement Sciences, Vrije Universiteit Amsterdam, the Netherlands
[b] Dept. of Rehabilitation Medicine, Amsterdam Movement Sciences, Amsterdam UMC, Vrije Universiteit Amsterdam, the Netherlands
[c] Dept. Biomechanical Engineering, Delft University of Technology, Delft, the Netherlands

ABSTRACT

Accurate assessment of the talo-crural (ankle) joint angle at physical examination is important for assessing extensibility of m. triceps surae (TS) in children with spastic cerebral paresis (SCP). The main aim of this study was to quantify foot flexibility during standardized measurements of TS muscle-tendon complex extensibility (i.e. based on foot-sole rotation) in SCP children, and typical developed (TD) ones. Additionally, we aim to define a method that minimizes the confounding effects of foot flexibility on estimates of talo-crural joint angles and TS extensibility.

Children, aged 6–13 years, with SCP (GMFCS I-III, n = 13) and TD children (n = 14) participated in this study. Externally applied -1 Nm, 0 Nm, 1 Nm and 4 Nm dorsal flexion foot plate moments were imposed. Resulting TS origin-insertion lengths, foot sole (φ_{FoSo}) rotations, and changes in talo-crural joint angle (φ_{TaCr}) were measured. Foot flexibility was quantified as $\Delta(\varphi_{TaCr} - \varphi_{FoSo})$ between the 0 Nm and 4 Nm dorsal flexion conditions.

In both groups, φ_{FoSo} rotations of approximately 20° were observed between 0 Nm and 4 Nm dorsal flexion, of which about 6° ($\approx$30%) was related to foot flexibility. Foot flexibility correlated to φ_{FoSo} (r = 0.69) but not to φ_{TaCr} (r = 0.11). For φ_{FoSo} no significant differences were found between groups at 4 Nm. However, for SCP children the mean estimate of φ_{TaCr} was 4.3° more towards plantar flexion compared to the TD group (p < 0.05). Normalized TS lengths show a higher coefficient of correlation with φ_{TaCr} ($r^2 = 0.82$) than with φ_{FoSo} ($r^2 = 0.60$), indicating that TS lengths are better estimated by talo-crural joint angles.

In both SCP and TD children aged 6–13 year, estimates of TS length and extensibility based on foot sole assessments are confounded by foot flexibility. Assessments of TS extensibility at physical examination will be more accurate when based on measurements of talo-crural joint angles.

© 2019 Published by Elsevier Ltd.

1. Introduction

Children with spastic cerebral paresis (SCP) often develop a limited ankle dorsiflexion range of motion, that impedes walking performance. This impairment may be caused by (1) hyper excitation and/or by (2) increased stiffness of TS or parts thereof and/or (3) relative shortening of the muscle-tendon complexes because of soft tissue adaptations (van den Noort et al., 2017; de Bruin et al., 2014), and/or (4) by interaction of TS with other muscles and tissues (Huijing and Baan, 2001).

Because of the anatomical specifics of the talo-crural joint, it is not easy to measure the talo-crural joint angle precisely during physical examination. In clinical practice, but also in sports sciences and in general in biomechanics (Honert and Zelik, 2016; Bobbert et al., 1986; Vinti et al., 2018), assessment on TS extensibility is commonly inferred from foot sole range of motion being interpreted as ankle joint range of motion. Typically, at physical examination, the examiner applies force on the forefoot driving the foot manually into dorsal flexion to test, either by observation (estimation) or by measurement (handheld goniometry or inclinometry), how much change in orientation of the foot sole is affected (Gracies et al., 2010; Tardieu, 1954). This is referred to as dorsal ankle range of motion and commonly interpreted as being related directly to TS extensibility (e.g. Weide et al., 2015). Note that such a proportional relation between TS extensibility and foot sole rotation, mostly implicitly, assumes a rigid foot (e.g. Tardieu et al., 1976).

---

* Corresponding author.

E-mail address: j.harlaar@amsterdamumc.nl (J. Harlaar).

Over the last 40 years several studies have shown that this assumption is violated because, the foot deforms internally upon application of external forces (Iwanuma et al., 2011; Tardieu et al., 1976; Wrbaškić and Dowling, 2007; Tardieu et al., 1977a; Carlson et al., 2000; Huijing et al., 2013; Bruening et al., 2012). Moreover, in SCP children, such foot flexibility was found to be more prominent when compared to that in developing (TD) children (Huijing et al., 2013; Tardieu et al., 1977a).

In view of the above, to allow accurate assessment of TS extensibility during physical examination, net effects of foot flexibility need to be accounted for. A method is needed to discriminate between foot sole rotation due to deformation within the foot and due to actual angular talo-crural joint changes. Such an approach has been proposed as early as 1977 by Tardieu et al. (1977a). They estimated talo-crural joint angular changes by correcting the foot sole angle with an estimate of foot flexibility.

Inspired by the approach by C. Tardieu, the aim of this study was to quantify foot deformations during standardized TS extensibility assessments in children with spastic cerebral paresis and compare results to those of typically developing children. Additionally, we aim to define a method that minimizes the confounding effects of foot flexibility on estimates of talo-crural joint angles.

2. Methods

2.1. Subjects

Thirteen children aged 6–13 years with uni- or bilateral Spastic Cerebral Paresis (SCP) (GMFCS I-III) (Palisano et al., 1997) were selected from a population visiting the Amsterdam University Medical Centre. Selected children for the SCP group had not undergone any surgical intervention of the muscles of the lower limb, nor chemical denervation (Botulinum toxin-A) 6 months prior to the measurements. A sample of typically developing children (TD) within the identical age range participated as the control group. In addition, for both groups, the presence of any other disease affecting the musculoskeletal system would exclude participation. Written informed consent for all participants from both parents was obtained. The study was approved by the ethics committee Amsterdam University Medical Centre.

For all subjects, measurements were performed by the same assessor at one leg. For the SCP group the leg yielding the most resistance to ankle dorsal flexion, while in the TD group, the right leg was selected.

2.2. Anthropometry

Body mass, body height, and foot length were measured. Lower leg length of the target leg was approximated as the mean of distances, measured medially and laterally, from the most prominent point of each femur epicondyle to the most prominent point of the corresponding malleolus. Mean malleoli height was defined as the mean of the distances measured medially and laterally from the most prominent point on the malleolus perpendicular towards the foot sole. These measurements were done using a 3D pointing stylus, tracked by a motion capture system (NDI Optotrak 3020).

2.3. Electromyography

In order to assess muscle excitation during inclino-dynamometry, as well as during foot sole and 3D stylus measurements, surface electromyography (EMG) of gastrocnemius lateralis and tibialis anterior muscles were collected (MOBI, TMS-International, The Netherlands). Preparation of the skin and placements of the EMG electrodes were performed according to

SENIAM instructions (Hermens et al., 1999). Using a multichannel system EMG signals were A/D converted at 1024 Hz and recorded synchronously on a PC. Prior to the measurements, participants were asked to perform a 5 s isometric maximal voluntary contraction (MVC, against resistance supplied by the assessor) towards dorsal and plantar flexion.

2.4. Inclino-dynamometer: Externally applied ankle moments induced foot plate angles

Subjects were lying prone on the examination table with both feet hanging over the edge (allowing free movements of the feet). The orientation of the selected foot was imposed using a custom designed apparatus (Bénard et al., 2010), comprising an adjustable foot plates and a torque wrench equipped with an inclinometer for angular measurements (this system will be referred to below as inclino-dynamometer) (Bénard et al., 2010; Huijing et al., 2013). The inclino-dynamometer was connected to the adjustable foot plate (Fig. 1A). Similar to the stabilization of the foot performed during physical examination, as well as during fitting of an ankle-foot orthoses, this foot plate allows adjustments targeted to stabilize the subtalar joint as much as possible during foot sole rotations (Huijing et al., 2013). In short: (1) Positioning of the calcaneus in a neutral position under the tibia. (2) Adduction of the forefoot until the midline of the calcaneus points between 2nd and 3rd ray of the forefoot. (3) Applying additional fore and mid-foot supination until no movement within the subtalar joint can be detected by palpation (Huijing et al., 2013). To ensure that we moved the foot sole into dorsal flexion within the sagittal plane we carefully moved the arm of the hand held inclino-dynamometer within the longitudinal orientation of the tibia.
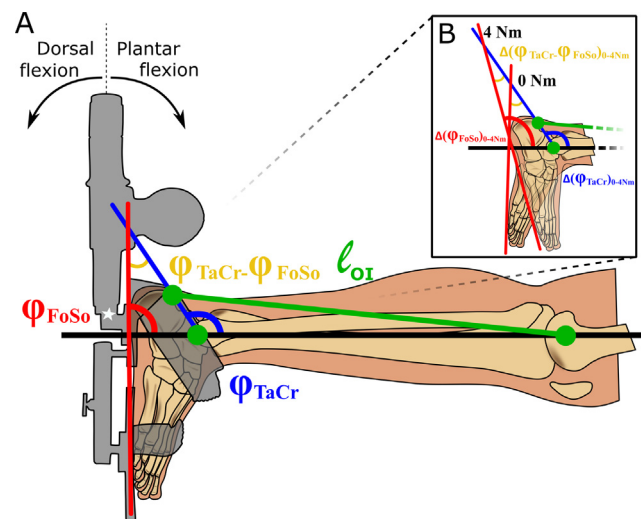

Fig. 1. Schematic representation of assessment of the foot and triceps surae length. A. Schematic representation of experimental setup: in grey inclino-dynamometer attached to the foot footplate. White star indicates the points of application of moments exerted. Red line: used in assessments of foot sole angle (φ_{FoSo}). Green line: origin to insertion length (ℓ_{OI}) of the triceps surae (TS). Blue line: estimated talo-crural joint angle (φ_{TaCr}). Green filled circles represent the anatomical landmarks from a sagittal perspective (i.e. medial and lateral femur epicondyles, medial and lateral malleoli and TS insertion on the calcaneus). The resultant angle colored in yellow between φ_{TaCr} and φ_{FoSo} represents the relative orientation of the line between the insertion and center of the bi-malleolar line with respect to the foot plate (φ_{TaCr} - φ_{FoSo}). B. Schematic representation of foot flexibility for a hypothetical situation in which foot flexibility Δ (φ_{TaCr} -φ_{FoSo})$_{0-4Nm}$ fully explains foot sole dorsal flexion Δ (φ_{FoSo})$_{0-4Nm}$ without any changes in talo-crural joint angle Δ (φ_{TaCr})$_{0-4Nm}$ and without changes in triceps surae length [Δ (ℓ_{OI})$_{0-4Nm}$] in response to 0–4 Nm externally applied moments. (For interpretation of the references to the colors in this figure legend, the reader is referred to the web version of this article.)

2.5. Foot sole angle and 3D stylus measurements

Foot sole angles were measured corresponding to externally applied dorsal flexion moments (i.e. −1 Nm, 0 Nm, 1 Nm and 4 Nm exerted to the foot plate). The angle of the foot sole was measured as the angle between the lateral rim of the foot sole (defined as the line between the most distal point at the lateral heel and the most distal point of the fifth metatarsophalangeal joint) and the lower leg (i.e. the line connecting the center of the bi-malleolar line and the center of the line connecting the femoral epicondyles) (Fig. 1). At each foot sole angle, 3D coordinates of bony-landmarks (i.e. medial and lateral femur epicondyles, medial and lateral malleoli and triceps surae muscle insertion on the calcaneus) were recorded using the 3D stylus measurements.

2.6. Data analysis

For each externally applied moment condition, foot sole angle, muscle-tendon complex length and estimates of talo-crural joint were calculated based on 3D pointer measurements. Angles of the foot sole and talo-crural joint were presented with a 90° offset, e.g. a foot sole angle of 0° corresponds to foot sole orientated perpendicular with respect to the lower leg. The distance related to the muscle-tendon complex length, was defined as the distance between the estimated muscle origin to the point of insertion (being referred to as origin-insertion distance (ℓ_{OI})), i.e. from the center of the line between the femur epicondyles to the location of insertion on the calcaneus). Note that this line does not necessarily have to pass through the muscle belly and tendon.

As a function of φ_{FoSo}, a third-order polynomial fit of muscle–tendon complex lengths, normalized for lower leg length, was made to allow comparison at identical φ_{FoSo} between subjects. Talo-crural joint rotation (φ_{TaCr}) was estimated as the difference in angle between the line connecting the Achilles tendon insertion to the center of the inter-malleolar line and the lower leg (Fig. 1A). Both values of φ_{TaCr} and φ_{FoSo} are presented as a deviation from their perpendicular orientation (i.e. an offset) with respect to the lower leg. Angle, angular changes and external moments in the dorsal direction are indicated as positive values.

We used a simple planimetric approach to compare φ_{TaCr} and φ_{FoSo} in the rotational plane (i.e. sagittal plane) (see Fig. 1). Our estimate of foot deformation is expressed as the difference between φ_{TaCr} and φ_{FoSo} measured at 0 Nm externally applied footplate moment: $(\varphi_{TaCr}\text{-}\varphi_{FoSo})_{0Nm}$. Net foot flexibility was defined as the change in $\varphi_{TaCr}\text{-}\varphi_{FoSo}$ between 0 Nm and 4 Nm externally applied moments $\Delta(\varphi_{TaCr}\text{-}\varphi_{FoSo})_{0\text{-}4Nm}$ (Fig. 1B).

EMG signals were high-pass filtered at 20 Hz, to eliminate movement artefacts; then rectified and subsequently low-pass filtered at 5 Hz, to get the linear envelope. MVC normalized EMG values were used to assess the amount of muscle excitation during the measurements. MVC normalized experimental results were discarded if low pass filtered MVC normalized EMG values from inclino-dynamometer and pointer measurements exceeded 10% of MVC. However, actual values measured during the experiments were considerably lower.

2.7. Statistics

For age, body mass, body height, lower leg length, foot length and malleoli height, a student t-test was used to test for significant differences between SCP and TD children. Two-Way mixed ANOVA with between subject factor (experimental group) and within subject factor (conditions: externally applied moment) was performed to test for interaction effects (group × condition) and main effects of group. Note that two participants could not be included in this

analysis because of missing data points (in 1 SCP participant the −1 Nm plantar flexion condition is missing and in 1 TD participant the 4 Nm dorsal flexion condition is missing).

Pearson's correlation regression analyses were used to determine correlation and direction of the linear relationship of foot deformation (i.e. $\varphi_{TaCr}\text{-}\varphi_{FoSo}$) and angles of the foot (i.e. φ_{TaCr} and φ_{FoSo}).

In order to evaluate the agreement between the TS extensibility measured directly (ℓ_{OI}) versus the estimated TS extensibility via the φ_{TaCr} or φ_{FoSo} assessments, we converted the data from all conditions to Z-scores (Z-score = (individual values-mean value of group)/SD). Agreements between TS extensibility (determined as normalized difference in l_{OI} between 0 Nm and 4 Nm) and the estimated TS extensibilities (i.e. Z-scores based on φ_{TaCr} and φ_{FoSo}) were assessed using Bland-Altman analysis (Bland and Altman, 1999). For all statistics we used SPSS (version 21.0, SPSS Inc., 2008). The level of significance was set at $p < 0.05$.

3. Results

3.1. Subject characteristics

Characteristics for SCP (GMFCS (Palisano et al., 1997) characterization I-III) and TD children are presented in Table 1. No significant mean differences between these groups were found. In addition, a distribution of SCP specific patient characteristics (GMFCS, uni/bi-lateral, foot) are presented in Table 1 for the SCP group.

3.2. Degree of muscle excitation

During measurements, normalized EMG activity was low (mean = 2.2% MVC) and not different between groups. In addition, all measurements were well below the criterion a priori set at 10% MVC. Therefore, we conclude that the results are not affected by muscle excitations.

3.3. Normalized TS origin-insertion length as a function of foot sole angles

Fig. 2 shows TS origin-insertion length normalized for lower leg length, as a function of foot sole angle. Note that mean values for $\ell_{OI}/\ell_{lowerleg}$ as a function of φ_{FoSo} for the SCP children are within the 95% confidence interval of the TD children (shaded area), and vice versa.

Table 1

Descriptive and anthropometric variables of SCP and TD children and a distribution of patient characteristics.

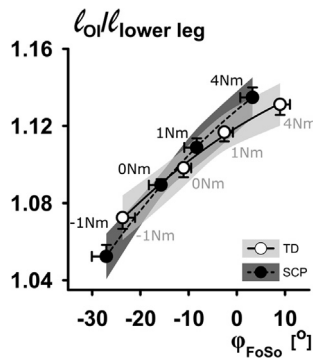|	SCP (n = 13) mean ± SE	TD (n = 14) mean ± SE
Age (years)	9.7 ± 0.6	9.3 ± 0.5
Body mass (kg)	33.2 ± 2.7	33.2 ± 2.7
Body Height (cm)	136.8 ± 3.5	140.5 ± 3.8
Lower leg length (cm)	31.2 ± 1.1	32.8 ± 1.2
Foot length (cm)	20.7 ± 0.7	20.7 ± 0.8
Malleoli height (cm)	7.9 ± 0.2	8.3 ± 0.2
Patient characteristics		
GMFCS (I/II/III)	(3/9/1)	NA
Foot (pesplanovalgus/pes planus/normal)	(5/5/3)	NA
Affected (unilateral/bilateral/unknown)	(2/10/1)	NA

Fig. 2. Normalized muscle-tendon complex length as function of foot sole angle. Mean values and SE of GM origin-insertion length, normalized for lower leg length ($\ell_{oi}/\ell_{lower\,leg}$), plotted as a function of foot sole angle (φ_{FoSo}) for groups of children with spastic cerebral palsy (SCP) and typically developed (TD) children. The shaded areas represent the 95% confidence intervals for TD and SCP groups.

3.4. Normalized TS origin-insertion length as a function of externally applied moments

Also, for changes in normalized TS origin-insertion length ($\ell_{OI}/\ell_{lowerleg}$) ANOVA showed a significant main effect for externally applied moments exclusively ($F(3,69) = 86.43$, $p < 0.01$). Note that, as there was no main effect of group ($F(1,23) = 2.56$, $p = 0.12$), nor a significant interaction effect ($F(3,69) = 2.1$, $p = 0.14$). This indicates that no distinction in normalized TS ℓ_{OI} between these groups can be made over the particular range of externally applied moments studied.

3.5. Foot sole and talo-crural joint changes

Fig. 3A shows values of φ_{FoSo} and φ_{TaCr} as a function of externally applied moments. For φ_{FoSo}, two-way mixed ANOVA showed neither a significant main effect (of groups) ($F(1,23) = 1.53$, $p = 0.23$), nor interaction ($F(3,69) = 0.14$, $p = 0.78$). Exclusively, a significant main effect of externally applied moments on φ_{FoSo}
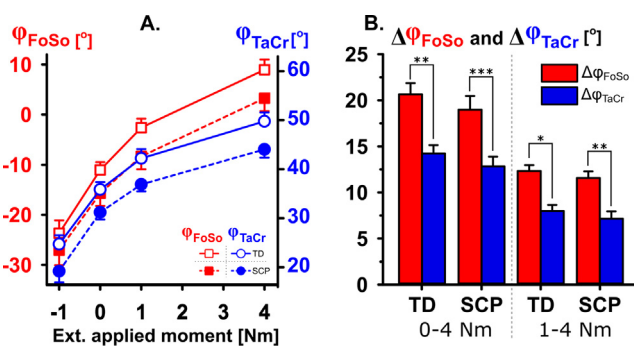

Fig. 3. Foot sole angle and estimated talo-crural joint orientation as a function of foot plate moments. A. For SCP and TD groups, the angle of foot sole (φ_{FoSo}; red, left Y-axis) with the longitudinal axis of the lower leg with, as well as the angle of the talo-crural joint (φ_{TaCr}; blue, right Y-axis) means values and SE are plotted as a function of externally applied moments (positive indicates dorsal flexion). Note that for both groups, angles corresponding to φ_{TaCr} and φ_{FoSo}, diverge with respect to each other, particularly at higher moments (>0 Nm). B. Between the externally applied moments of 0–4 Nm and 1–4 Nm, bar graphs showing for each group separately values (mean and SE) for differences between subsequent data points of angles φ_{FoSo} and φ_{TaCr}, respectively. Differences have been calculated for φ_{FoSo} and φ_{TaCr} separately. The changes in φ_{TaCr} were smaller than those in φ_{FoSo}, particularly differences measured between 0 Nm and 4 Nm external moment. * indicates significant differences at $p < 0.05$; ** and *** indicate significance at $p < 0.01$ and $p < 0.001$, respectively. All data are presented as mean values (and SE). (For interpretation of the references to color in this figure legend, the reader is referred to the web version of this article.)

was found ($F(3,69) = 197.72$, $p < 0.01$). These findings show that the present two groups cannot be distinguished statistically based on φ_{FoSo} changes in response to externally applied moments.

For φ_{TaCr}, ANOVA showed no interaction effects ($F(3,69) = 0.20$, $p = 0.71$) between main factors, however it did show a main effect of group: the φ_{TaCr} curve having shifted 4.3° more towards plantar flexion for the SCP group compared to the TD group ($F(1,23) = 5.54$, $p = 0.03$). In addition, ANOVA showed main effects of externally applied moments for φ_{TaCr} ($F(3,69) = 133.45$, $p < 0.01$).

In summary, at similar externally applied moments, the corresponding values for φ_{TaCr} were more towards plantar flexion in the SCP group, however $\Delta(\varphi_{TaCr})_{0-4Nm}$ over the range of externally applied moments was not different between groups. In conclusion, between groups, no differences in changes of φ_{FoSo} and φ_{TaCr} over the range of externally applied moments were found.

3.6. Foot deformation

Fig. 3A + B shows that between 0 and 4 Nm externally applied dorsal flexion moments φ_{FoSo} increased more compared to φ_{TaCr}. Note that for both groups, lines corresponding to φ_{FoSo} and φ_{TaCr}, diverge with respect to each other, particularly at higher moments (at >0 Nm) (Fig. 3A). Upon dorsal flexion of the foot by increasing externally applied moments from 0 Nm to 4 Nm, dorsal flexion range, $\Delta(\varphi_{FoSo})_{0-4Nm}$ exceeded $\Delta(\varphi_{TaCr})_{0-4Nm}$ This indicates that with higher applied moments, deformations within the foot increased. In both groups, φ_{FoSo} rotations of approximately 20° were observed between 0 Nm and 4 Nm dorsal flexion, of which about 6° ($\approx$30%) was related to foot flexibility. Since the value of foot sole rotation exceeds the value of talo-crural joint rotation in both groups, it is concluded that foot flexibility $\Delta(\varphi_{TaCr}-\varphi_{FoSo})$ occurs in both groups. In addition, since values of $\varphi_{TaCr}-\varphi_{FoSo}$ over the range of externally applied moments are not different between groups, we cannot conclude foot flexibility to be more prominent in the SCP group compared to the TD group.

3.7. Individual variation in foot sole rotation is largely explained by individual variation in foot deformation

Although no difference in $\varphi_{TaCr}-\varphi_{FoSo}$ could be shown between groups, regression analysis shows that individual values of $(\varphi_{TaCr}-\varphi_{FoSo})_{0\,Nm}$ were correlated to $(\varphi_{FoSo})_{0Nm}$ values ($r = -0.67$, Fig. 4A). This is a surprising effect, indicating that at 0 Nm external moment, individuals who have flatter foot (i.e. smaller values of $(\varphi_{TaCr}-\varphi_{FoSo})_{0\,Nm}$, attain a more dorsal flexed foot sole at 0 Nm external moment exerted $(\varphi_{FoSo})_{0\,Nm}$. In addition, regression analysis showed that higher negative values of $\Delta(\varphi_{TaCr}-\varphi_{FoSo})_{0-4\,Nm}$ (i.e. more flexible foot) corresponded to a larger range of foot sole motion ($r = -0.69$) (i.e. higher values of $\Delta(\varphi_{FoSo})_{0-4\,Nm}$, Fig. 4B). These results indicate that individuals exhibiting more dorsal flexion of the foot sole also show more foot flexibility over the moment range studied. In other words, subjects with both a high value of φ_{FoSo} at 0 Nm, as well as high value of $\Delta\varphi_{FoSo}$ between 0 Nm and 4 Nm, were most likely the subjects with flatter and more flexible feet. Note that for φ_{TaCr}, in contrast to φ_{FoSo}, no such effects for flexibility were found (Fig. 4CD).

3.8. Estimates for origin-insertion length changes

Fig. 5 shows for Z-scores of normalized origin-insertion length a higher coefficient of correlation with Z-scores of φ_{TaCr} ($r^2 = 0.82$) than with Z-scores of φ_{FoSo} ($r^2 = 0.60$). This indicates that changes in origin-insertion lengths are better estimated by changes in
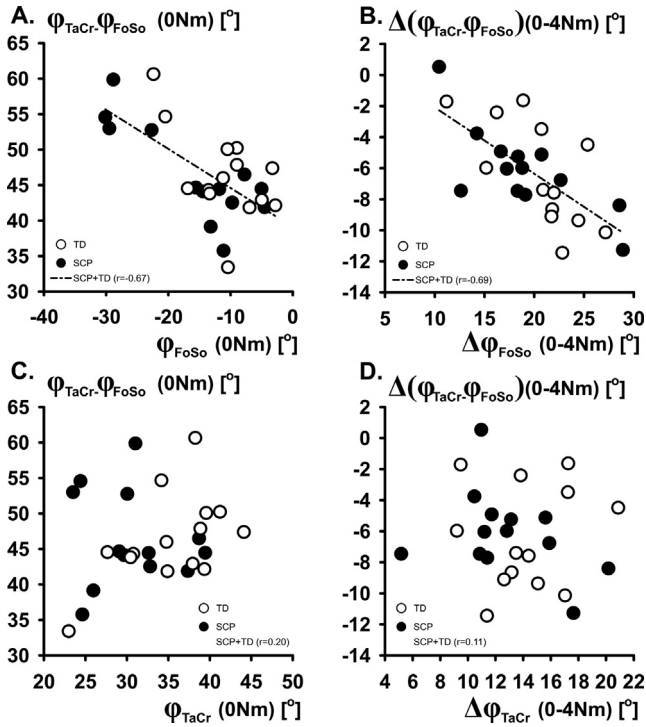
Fig. 4. Individual values of foot deformation plotted as functions of several angular variables of foot and ankle Left hand panels (i.e. A and C): Foot deformation values at exertion of 0 Nm externally applied moment as a function of angular variables of foot (A) and ankle (C). A. Foot deformation (φ_{TaCr} -φ_{FoSo}) plotted as a function of foot sole angle (φ_{FoSo}). C. Foot deformation (φ_{TaCr} -φ_{FoSo}) plotted as a function of talo-crural ankle joint angle (φ_{TaCr}). Right hand panels (i.e. B and D): Foot flexibility in response to 0–4 Nm ($\Delta (\varphi_{TaCr} -\varphi_{FoSo})_{0-4Nm}$) as a function of angular variables of foot (B) and ankle (D). B. Foot flexibility as a function of changes in foot sole angle $\Delta (\varphi_{FoSo})_{0-4Nm}$. D. Foot flexibility as a function of changes in talo-crural ankle joint angle $\Delta (\varphi_{TaCr})_{0-4Nm}$. Note that panel B shows that subjects with larger dorsal flexion foot sole ranges between 0 and 4 Nm display increased foot flexibility. In addition, panel D shows that increases in talo-crural ankle joint range of motions, between 0 Nm and 4 Nm, were not related to increases in foot flexibility, whatsoever.

Fig. 5. Foot angular predictors of triceps surae (TS) lengths. A. Z-scores of normalized TS origin-insertion length (loi/lowerleg) as a function of Z-scores of foot angles, i.e. foot sole angle (φ_{FoSo} red squares) and talo-crural joint angles (φ_{TaCr} blue circles). The grey dotted line indicates the line of identity. B. Bland-Altman plot of Z-score differences between foot angle (φ_{FoSo} red squares, φ_{TaCr} blue circles) and TS length as a function of the mean Z-score between foot angle and TS length. Blue and red dotted lines represent the 95% confidence interval of φ_{FoSo} and φ_{TaCr}, respectively. (For interpretation of the references to color in this figure legend, the reader is referred to the web version of this article.)

talo-crural joint angles compared to changes in foot sole angles. Moreover, Bland-Altman analysis (Fig. 5) shows a better agreement between normalized origin-insertion lengths data and φ_{TaCr} than

between normalized muscle-tendon complex lengths and φ_{FoSo}. Therefore, it is concluded that assessment of the talo-crural joint angle improves estimation of triceps surae muscle origin-insertion lengths.

4. Discussion

In clinical and scientific work, assessments of TS extensibility is difficult because the talo-crural joint angle is not easily measured. A practical approach used to asses TS extensibility has been to assume a direct relation of foot sole rotation with TS extensibility. However, deformation of the foot (i.e. the forefoot rotating relative to the hindfoot) confounds TS extensibility assessments by allowing enhanced foot sole dorsal flexion at the midfoot.

Using a straightforward geometrical approach, we found that for both the SCP and TD groups, up to 30% of foot sole rotations was obtained by dorsal flexion within the foot, rather than at the talo-crural joint (φ_{TaCr}). Taking into account foot geometry and its changes provide insight in effects of foot flexibility on TS extensibility. This suggests that TS extensibility, if to be inferred from foot manipulations and likely also gait kinematics, should be based on measurements or estimates of talo-crural angular changes ($\Delta\varphi_{TaCr}$) and not on foot sole angular changes ($\Delta\varphi_{FoSo}$). To obtain estimates of moment arm at the talo-crural joints based on angular changes and muscle-tendon complex length changes, the use of $\Delta\varphi_{TaCr}$ is advised.

4.1. Foot deformation in SCP and TD children

With regard to foot deformation in relation to TS length and extensibility, two elements can be distinguished: (1) differences in foot geometry present when no external moment is applied (i.e. static, described as static foot deformation) and (2) added deformation within the foot in response to higher externally applied moments (i.e. deformation, described here as foot flexibility). Previously, using ultrasound imaging methods, it was shown that muscle-tendon lengths even if normalized for lower leg length, at equal footplate angles were smaller in SCP children compared to that of TD children (Huijing et al., 2013). In addition, based on X-rays, that study also found that in a child with SCP deformation of the foot was twice that of a TD subject (Huijing et al., 2013). Excellent studies by the group of Tabary and Tardieu in the 1970's did indicate that foot flexibility needs to be considered to obtain adequate estimates of the triceps surae extensibility in children with SCP (e.g. Tardieu et al., 1977b). We showed that in SCP children dorsal flexion within the mid foot occurs. However, contrary to our expectation, ANOVA did not show differences between SCP and TD groups, neither for static foot deformation nor foot flexibility. This may be related to our limited group size in the presence of high individual variation, but also to the fact that SCP children in this study were only mildly affected, i.e. less than in previous work. We were anticipating a more compliant subtalar joint in children with SCP, so our targeted stabilization of the subtalar part of the hind foot (see method) may also have been successful to decrease foot flexibility in children with SCP to equal extents compared to TD children. Further research is needed to quantify how effects of stabilization or repositioning bones constituting the foot affects foot deformities in SCP children. Altogether, we found 30% differences between $\Delta\varphi_{FoSo}$ and $\Delta\varphi_{TaCr}$ rotations, indicating that foot flexibility in both SCP and TD children was apparent.

4.2. Typical assessments of TS extensibility and flexibility of the foot

In a common clinical setting, although attempts are made to stabilize the foot, TS extensibility assessments based on foot sole
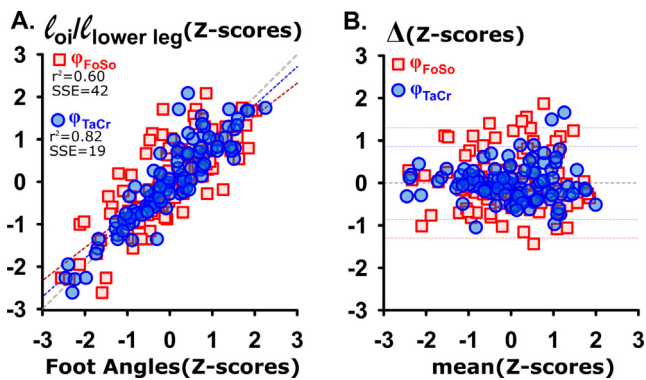
rotation are biased by foot flexibility. The relation between angular change of the foot sole and TS extensibility has been shown in cadaveric tendon excursion studies (Grieve et al., 1978). Note that because the Achilles tendon was cut in that study, driving the foot into dorsal flexion can be done at low force (i.e. without the need to stretch the TS) so it evokes limited or no foot flexibility in fixed preparations compared to in-vivo or in-situ experiments. Maybe because of this, numerous studies aiming to assess TS length or its extensibility ignored effects of foot flexibility and confused foot sole angle with ankle angle (Weide et al., 2015; Kawakami et al., 2008; Muraoka et al., 2005).

Moreover, in the intact ankle-foot complex, forces that are applied on the foot in cadaveric experiments lead to sizeable (spring like) flexion or extension within the foot (Ker et al., 1987). So far only a few studies have addressed foot flexibility during low activity dynamic TS extensibility assessments *in-vivo* (Iwanuma et al., 2011; Tardieu et al., 1977a; Huijing et al., 2013). Variations in flexibility of the foot are likely related to variations in both length, and stiffness of muscles and ligamentous structures connecting the 28 bones within the foot (Mosca, 2010). In addition, variation in foot deformation may have also contributed to foot flexibility because of joint sub-luxation allowing non-physiological degrees of freedom. Large variations related to foot flexibility complicate clinician's efforts to stabilize the foot in order to apply TS extension without additionally dorsal flexing and/or pronating or supinating the foot. Further studies are needed to develop methods, simple enough for clinical application, that aid clinicians to assess and apply TS extension without the confounding effects of foot flexibility.

4.3. Limitations of the estimate of the talo-crural joint angle

TS extensibility in response to dorsal flexion moments is related primarily to rotation within the sagittal plane at the talo-crural joint axis that lengthens TS. We defined changes in the talo-crural joint as the changes in orientation of the line connecting the Achilles tendon insertion and the center of the inter-malleolar line, with respect to the lower leg. Since angular changes will also be affected by movement of the calcaneus relative to the talus or translation of the malleoli with respect to the talus, our estimate is not strictly an estimator of the talo-crural joint movements exclusively. The suggested estimate of talo-crural joint rotation provides an intuitive approach to estimate talo-crural ankle joint angles without the use of X-ray or fluoroscopy allowing to measure more subjects. However, not all individual TS lengths could be explained by estimated talo-crural joint angles, which besides measurement noise, could be related to variations in moment arm lengths and as the talo-cural joint axis is likely to translate due to specific articulating bone surfaces it could also be related to inaccurate assessments of the joint axis (Lundberg et al., 1989). Incorrect placements of the line connecting the insertion and malleoli, to estimate φ_{TaCr} will introduce inaccuracies. Nevertheless, our estimate of TS extensibility based on talo-crural joint rotation is an improvement over foot sole based measurements.

5. Conclusion

It is concluded that for the foot dorsal flexion range studied, internal foot mechanics have a substantial effect on foot sole angles attained particularly at higher externally applied dorsal flexion moments. Therefore, estimates of triceps surae muscle length changes based on interpretation of foot sole angles are not accurate, and should be based on the talo-crural joint angles or assessment of TS length instead. Further investigations are war-ranted to study underlying mechanisms of foot deformation and flexibility, particularly in children with spastic cerebral paresis. In addition, further research before implementation is required to design concrete guidelines for assessment of talo-crural joint rotations during clinical examinations.

Declaration of Competing Interest

The authors declares that there are no conflicts of interest.

Acknowledgements

References

Bénard, M.R. et al., 2010. Reproducibility of hand-held ankle dynamometry to measure altered ankle moment-angle characteristics in children with spastic cerebral palsy. Clin. Biomech. 25, 802–808.

Bland, J.M., Altman, D.G., 1999. Measuring agreement in method comparison studies. Stat. Methods Med. Res. 8, 135–160.

Bobbert, M.F., Huijing, P.A., van Ingen Schenau, G.J., 1986. A model of the human triceps surae muscle-tendon complex applied to jumping. J. Biomech. 19, 887–898.

Bruening, D.A., Cooney, K.M., Buczek, F.L., 2012. Analysis of a kinetic multi-segment foot model part II: kinetics and clinical implications. Gait Posture 35, 535–540.

de Bruin, M. et al., 2014. Intramuscular connective tissue differences in spastic and control muscle: a mechanical and histological study Sampaolesi M, ed. PLoS One 9, e101038.

Carlson, R.E., Fleming, L.L., Hutton, W.C., 2000. The biomechanical relationship between the tendoachilles, plantar fascia and metatarsophalangeal joint dorsiflexion angle. Foot Ankle Int. 21, 18–25.

Gracies, J.M. et al., 2010. Five-step clinical assessment in spastic paresis. Eur. J. Phys. Rehabil. Med. 46, 411–421.

Grieve, D.W., Pheasant, S., Cavanagh, P.R., 1978. Prediction of gastrocnemius length from knee and ankle joint posture. Biomech. VI-A 2, 405–412.

Hermens, H.J., Disselhorst-Klug, C., Rau, G., 1999. The recommendations for sensors and sensor placement procedures for surface electromyography. In: Hermens, H., Freriks, B., Merletti, R., et al. (Eds.), SENIAM 8; European Recommendations for Surface Electromyography. Roessingh Research and Development B.V.Volln Seniam. pp. 13–54.

Honert, E.C., Zelik, K.E., 2016. Inferring muscle-tendon unit power from ankle joint power during the push-off phase of human walking: insights from a multiarticular EMG-Driven ModelIvanenko YP, ed. PLoS One 11, e0163169.

Huijing, P.A. et al., 2013. Movement within foot and ankle joint in children with spastic cerebral palsy: a 3-dimensional ultrasound analysis of medial gastrocnemius length with correction for effects of foot deformation. BMC Musculoskelet. Disord. 14, 365.

Huijing, P.A., Baan, G.C., 2001. Myofascial force transmission causes interaction between adjacent muscles and connective tissue: effects of blunt dissection and compartmental fasciotomy on length force characteristics of rat extensor digitorum longus muscle. Arch. Physiol. Biochem. 109, 97–109.

Iwanuma, S. et al., 2011. Triceps surae muscle-tendon unit length changes as a function of ankle joint angles and contraction levels: the effect of foot arch deformation. J. Biomech. 44, 2579–2583.

Kawakami, Y., Kanehisa, H., Fukunaga, T., 2008. The relationship between passive ankle plantar flexion joint torque and gastrocnemius muscle and achilles tendon stiffness: implications for flexibility. J. Orthop. Sport. Phys. Ther. 38, 269–276.

Ker, R.F. et al., 1987. The spring in the arch of the human foot. Nature 325, 147–149.

Lundberg, A. et al., 1989. The axis of rotation of the ankle joint. J. Bone Jt. Surgery, Br. 71-B, 49–99.

Mosca, V.S., 2010. Flexible flatfoot in children and adolescents. J. Child. Orthop. 4, 107–121.

Muraoka, T. et al., 2005. In vivo passive mechanical properties of the human gastrocnemius muscle belly. J. Biomech. 38, 1213–1219.

van den Noort, J.C. et al., 2017. European consensus on the concepts and measurement of the pathophysiological neuromuscular responses to passive muscle stretch. Eur. J. Neurol. 24. 981-e38.

Palisano, R. et al., 1997. Development and reliability of a system to classify gross motor function in children with cerebral palsy. Dev. Med. Child Neurol. 39, 214–223.

Tardieu, C. et al., 1976. An apparatus and a method for measuring the relationship of triceps surae to tibio-tarsal angles in man. Eur. J. Appl. Physiol. Occup. Physiol. 35, 11–20.

Tardieu, C. et al., 1977a. Relationship of triceps surae torques to photographed tibia-calcaneum angles in man (II). Eur. J. Appl. Physiol. Occup. Physiol. 37, 153–161.

Tardieu, G., 1954. A la recherche d'une technique de mesure de la spasticite. Rev. Neurol. 91, 143–144.

Tardieu, G., Lespargot, A., Tardieu, C., 1977b. To what extent is the tibia-calcaneum angle a reliable measurement of the triceps surae length? Radiological correction of the torque-angle curve (III). Eur. J. Appl. Physiol. Occup. Physiol. 37, 163–171.

Vinti, M. et al., 2018. Muscle shortening and spastic cocontraction in gastrocnemius medialis and peroneus longus in very young hemiparetic children. Biomed Res. Int.

Weide, G. et al., 2015. Medial gastrocnemius muscle growth during adolescence is mediated by increased fascicle diameter rather than by longitudinal fascicle growth. J. Anat. 226, 530–541.

Wrbaškić, N., Dowling, J.J., 2007. An investigation into the deformable characteristics of the human foot using fluoroscopic imaging. Clin. Biomech. 22, 230–238.